North Pacific Gyre Oscillation modulates seasonal timing and ecosystem functioning in the California Current upwelling system

F. Chenillat,[1] P. Rivière,[1] X. Capet,[2] E. Di Lorenzo,[3] and B. Blanke[2]

Received 12 October 2011; revised 30 November 2011; accepted 7 December 2011; published 14 January 2012.

[1] On interannual and longer time scales, dynamical and biogeochemical fluctuations in the North Pacific are dominated by two modes of variability, namely the Pacific Decadal Oscillation and the North Pacific Gyre Oscillation (NPGO). In this study the regional expression of the NPGO in the California Current System (CCS) is detailed. The statistical relationship between the NPGO index and nearshore wind variability (mostly upwelling favorable) along the U.S. West coast is strongest in the wintertime (December to March) off Central California. Most importantly, NPGO fluctuations are associated with a seasonal shift of 1–2 months in the onset of the upwelling season. Regional numerical simulations show that an early (late) onset of upwelling during the positive (negative) phase of the NPGO leads to a more (less) productive planktonic ecosystem throughout spring and summer, i.e., several months after the direct NPGO effects on the system have ceased. These results bring new light on the California ecosystem variability as observed in atypical years such as 2005 and 2007. **Citation:** Chenillat, F., P. Rivière, X. Capet, E. Di Lorenzo, and B. Blanke (2012), North Pacific Gyre Oscillation modulates seasonal timing and ecosystem functioning in the California Current upwelling system, *Geophys. Res. Lett.*, *39*, L01606, doi:10.1029/2011GL049966.

1. Introduction

[2] The climate system is always changing and this large scale variability in time and space of the ocean-atmosphere system can be characterized by different modes of variability. A mode of variability is a specific pattern that presents identifiable characteristics, a regional signature and a long-term oscillatory behavior. Oscillations of only one mode or combined modes of variability are useful to rationalize observed climate fluctuations. They are also increasingly helpful to understand regional climate.

[3] Two oceanic climate patterns dominate in the North Pacific: the Pacific Decadal Oscillation (PDO) [*Mantua et al.*, 1997] and the recently identified North Pacific Gyre Oscillation (NPGO) [*Di Lorenzo et al.*, 2008]. The PDO is the leading mode of sea surface temperature (SST) variability and is connected to the El Niño Southern Oscillation (ENSO) [*Alexander et al.*, 2002]. The NPGO is the second mode of sea surface height anomalies (SSHa). It is associated with changes in strength of the central and eastern parts of the North Pacific gyre [*Di Lorenzo et al.*, 2008] and is the oceanic expression of the North Pacific Oscillation (NPO) [*Chhak et al.*, 2009; *Di Lorenzo et al.*, 2009], an atmospheric mode of variability that captures an important fraction of wintertime storm track variability [*Linkin and Nigam*, 2008] and which is also known to be linked with the central Pacific El Niño [*Di Lorenzo et al.*, 2010] - a different flavor of El Niño that has become more frequent in the last decades (see *Ashok et al.* [2009] for a review). The NPGO explains a significant fraction of interannual to decadal salinity, nutrient and chlorophyll-*a* (Chl-a) variance off the United States (US) West Coast [*Di Lorenzo et al.*, 2008, 2009]. There are strong indications that the relationship between the NPGO index and fluctuations of salinity, nitrate and Chl-a concentrations along the US West Coast is related to a modulation of upwelling favorable winds [*Di Lorenzo et al.*, 2008]. The details of this modulation are unknown and are the main subject of this study: our main result is that the NPGO is robustly associated with a modulation of the timing of the upwelling season (lag in upwelling onset) off the central part of the California Current System (CCS).

[4] Numerous recent studies dedicated to the CCS have reported that the upwelling onset, also called the "Spring transition", is a key factor for marine biology [*Bograd et al.*, 2009]. Interannual variability (or possibly long-term variability in relation with global climate change) of the spring transition timing has important biological consequences on the timing of nutrient input to the coastal system, with implications that propagate up the food chain (match/mismatch mechanisms) and an effect on the overall productivity of the system [*Barth et al.*, 2007].

[5] In this study, we clarify the statistical relationship between the NPGO index and the variability of upwelling favorable winds along the US West coast, based on alongshore wind patterns (section 2) and upwelling indices derived from station measurements (section 3). We find a clear link between NPGO and the timing of the spring transition. Because of the importance of regional changes in phenology (in particular in the context of climate change) we investigate numerically the ecosystem response of the CCS to a modulated upwelling season onset in relation with the NPGO (section 4). We show that the timing of the upwelling onset has important implications on the response of the California Current Ecosystem throughout the year. These results bring new insight into the functioning of the California ecosystem, especially for atypical years such as

[1]Laboratoire des Sciences de l'Environnement Marin, UMR 6539, Université de Bretagne Occidentale, Institut Universitaire Européen de la Mer, Plouzané, France.
[2]Laboratoire de Physique des Océans, UMR 6523, Université de Bretagne Occidentale, IFREMER, Brest, France.
[3]School of Earth and Atmospheric Sciences, Georgia Institute of Technology, Atlanta, Georgia, USA.

0094-8276/12/2011GL049966

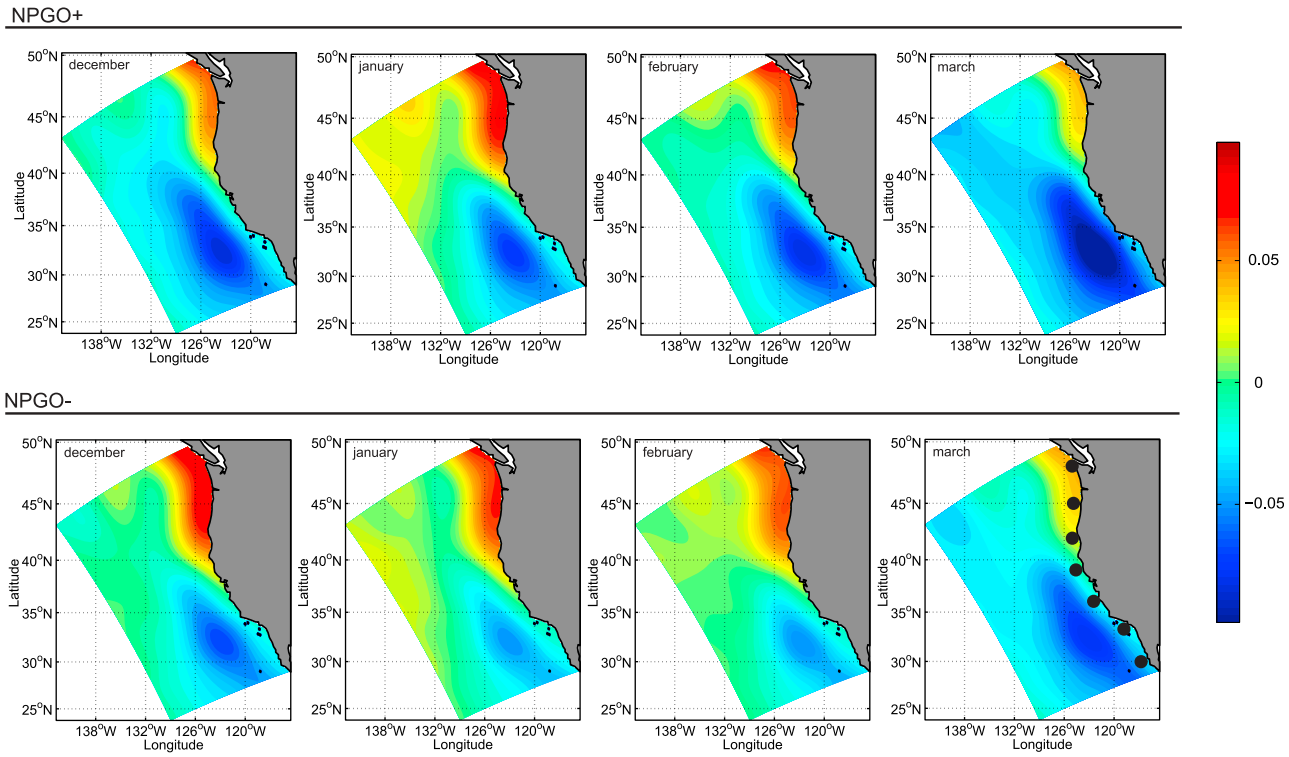

Figure 1. Monthly-mean alongshore winds from December to March NNR data for the (top) positive and (bottom) negative phases of the NPGO. Positive values represent poleward winds. Units are in N m^{-2}. Black points in the bottom right panel locate the stations from 30°N to 48°N where upwelling indices are computed. The 27°N station is not shown.

2005 and 2007 characterized by abnormal upwelling onset timings. Concluding remarks are given in section 5.

2. Variability of Alongshore Winds Patterns

[6] The relationship between seasonal variability of the upwelling and the NPGO is first investigated with alongshore wind observations. Wind data are taken from National Centre for Environmental Prediction/National Centre for Atmospheric Research Reanalysis (NNR) [*Kalnay et al.*, 1996]. Monthly-mean values available from 1950 to 2008 are gridded onto a 15 km by 15 km latitude/longitude grid rotated in the mean direction of the central US West Coast (Figure 1). It is known that these alongshore winds are significantly correlated with the NPGO index over the past 50 years [see *Di Lorenzo et al.*, 2008, Figure 1].

[7] First, we identify in the low-pass filtered NPGO index (two-year running mean) the years that unambiguously correspond to a NPGO+ or NPGO− situation as those for which the index does not change sign during the entire year. We count a total of 20 (NPGO+) and 25 (NPGO−) such years. Then, we compute NNR wind climatologies for these unambiguous NPGO+ and NPGO− years. Throughout winter, a dipole pattern emerges, irrespective of the NPGO phase (Figure 1). This dipole is characterized by a central-southern core of upwelling favorable winds, centered around (32.5°N, 123°W), and a northern core of downwelling favorable winds north of 48°N close to the coast. Although the boundary between both regions is slightly more southward in NPGO− than in NPGO+, the main difference between the two phases is noticeably the strength of the cores rather than their spatial extension: the core of upwelling (downwelling) favorable winds is about 2 times stronger (weaker) in NPGO+ than in NPGO−. Given the seasonality of the wind, this difference in magnitude translates into a lag of upwelling favorable winds between the two phases illustrated by the strong resemblance between the February NPGO+ and March NPGO− upwelling wind patterns.

[8] For every month and each NPGO phase, alongshore winds are averaged over the upwelling favorable wind region and we estimate the statistical significance of the differences between the two resulting climatologies with a non-parametric test [*Kruskal and Wallis*, 1952]. Winds are significantly different in wintertime, i.e., from December to March in the central and in the southern region of the CCS (no significant difference is observed in the northern CCS). The underlying mechanism responsible for this connection between the NPGO and the strength of winter upwelling winds is not evidently related to a change in winter storm activity. In particular, regression maps of 500 and 800 hPa atmospheric wind synoptic variability against the NPGO index do not reveal any storm track variability that could explain it. The rest of the year, wind differences between NPGO+ and NPGO− years are not statistically significant, although upwelling winds tend to be stronger year round in NPGO+ compared to NPGO− phase (see next section).

3. Seasonal Variability of the Upwelling

[9] The upwelling strength can be estimated by the coastal upwelling index (UI) [*Bakun*, 1973; *Schwing et al.*, 1996]. The UI represents a measurement of the volume of water that upwells (positive values) or downwells (negative values) at the coast, owing to coastal divergence of geostrophic winds.

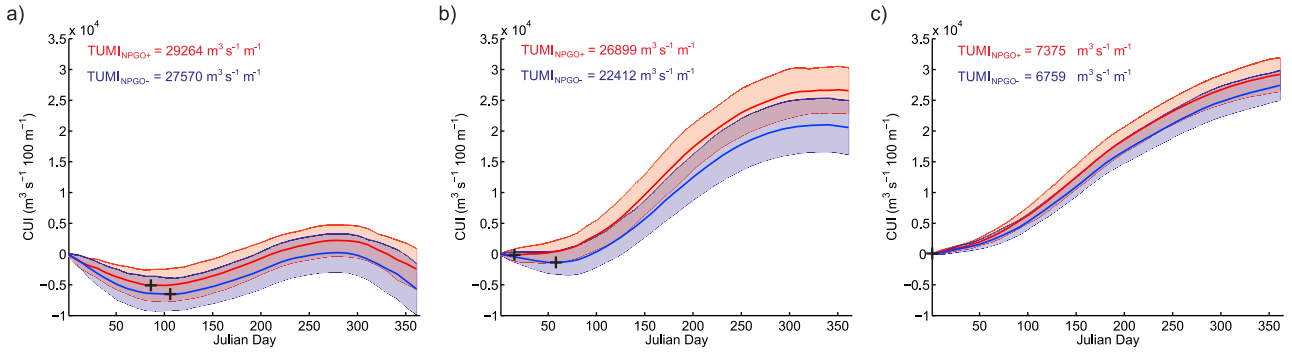

Figure 2. Cumulative Upwelling Index (CUI) for the positive (red) and negative (blue) phases of the NPGO, for (a) the northern, (b) the central and (c) the southern CCS. The mean and standard deviation are shown with a bold line and a shaded area, respectively. The Spring Transition Indexes are identified with black crosses.

Daily upwelling indexes based on surface atmospheric pressure fields with a 6-hourly, 1° resolution are provided by the US Navy Fleet Numerical Meteorology and Oceanography Center from 1967 to present, at 3-degree-distant stations along the US West Coast.

[10] Here, we explore daily UI time series at eight stations from 27°N to 48°N (Figure 1, bottom right). For any given year, the Cumulative UI (CUI) is calculated each day as the time integral of the UI from January 1st to this day [*Schwing*, 1996]. The CUI is useful because it smoothes out the synoptic variability of the upwelling forcing and helps reveal seasonality differences from year to year. Given our results in section 2, we are mainly interested in the early part of the seasonal cycle. Following *Schwing et al.* [1996], we also compute the spring transition index (STI) which characterizes, for any given year, the timing of the onset of the upwelling system and is defined as the time in days from January 1st to the day when the minimum value of the CUI is reached. We also make use of the overall intensity of the upwelling, the Total Upwelling Magnitude Index (TUMI), defined as $TUMI = \int_{STI}^{END} CUI \cdot dt$ where *END* is the end of the upwelling season characterized by the day when the CUI reaches its maximal value.

[11] We separate the CCS into three subregions separated by Point Conception and Cape Blanco and characterized by well-defined physical and biological oceanographic properties: the southern CCS (stations from 27°N to 33°N), the central CCS (stations from 36°N and 39°N) and the northern CCS (stations from 42°N to 48°N). For each subregion, we compute two climatological CUIs based on the same decomposition into NPGO+ and NPGO− years described in section 2.

[12] The NPGO+ CUI is consistently larger than the one for NPGO− (Figure 2) although the significance of these differences varies with the season and the subregion of the CCS. In the central CCS, the mean CUI profiles of NPGO+ and NPGO− are statistically different all year round as indicated by a non-parametric test [*Kruskal and Wallis*, 1952]. Compared to NPGO−, the NPGO+ upwelling season begins around 45 days earlier and the TUMI is about 20 % greater. Differences are less marked for the southern and northern CCS. In the southern CCS, the CUI climatologies for NPGO+ and NPGO− are not statistically different during the first 45 days of the year with an upwelling season that starts on January 1st (i.e., STI = 1) both for NPGO+ and NPGO− years. However, the TUMI is significantly greater in NPGO+ than in NPGO−, showing that the cumulative

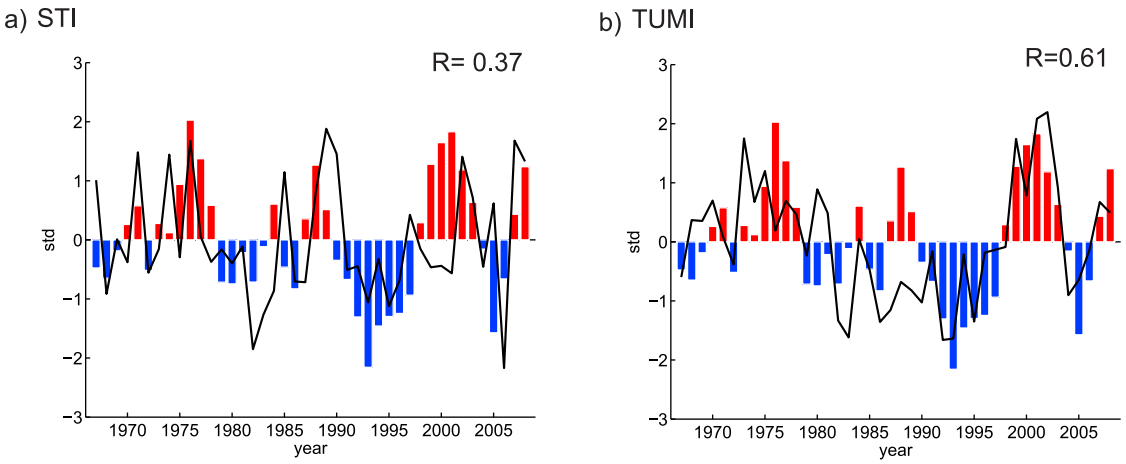

Figure 3. Comparison of the NPGO index (bar) with (a) the Spring Transition Index time series (reversed sign, line) and (b) the Total Upwelling Magnitude Index time series (line), both computed for the central CCS. The NPGO index is yearly averaged and normalized by its standard deviation. The STI and the TUMI have been also normalized by their standard deviation (std_{STI} = 27 days and std_{TUMI} = 3646 m^3 s^{-1} 100 m^{-1}). All correlations are significant at the 95% level or greater.

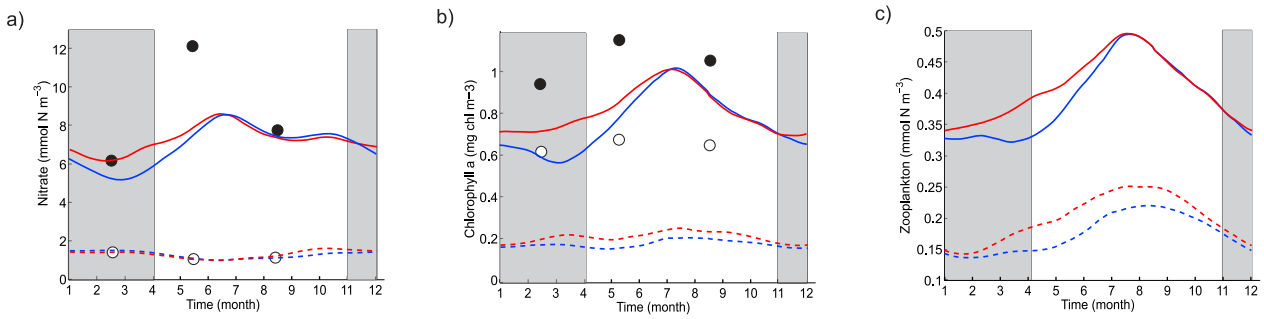

Figure 4. Temporal evolution of (a) nutrient, (b) total Chl-a and (c) total zooplankton concentrations in the model, of the simulations run in parallel for the NPGO+ (in red) and NPGO− (in blue) scenarios. The concentrations are averaged off central CCS in a near-shore region (solid lines) and an offshore region (dotted lines) (see text for details). The months when the winds differ between the two NPGO scenarios are shaded. Black and white dots represent coastal and offshore concentrations of nutrient and Chl-a, respectively, as derived from the seasonal mean of CalCOFI climatology line 70 data (1949–2000) averaged over the same depth and distance from the coast as the model outputs. Because Chl-a data along line 70 only go 350 km offshore, they are linearly extrapolated over an additional 100 km (to reach the western edge of the offshore box) using a slope coefficient deduced from the SeaWIFS Chl-a climatology over the same domain.

upwelling in NPGO+ is about 5 % more intense than in NPGO−. In the northern part of the CCS, the mean CUI profiles never differ statistically; all year round, TUMI and STI are thus considered the same for both NPGO phases. There is no evidence of changes in upwelling variability with the NPGO in the northern CCS.

[13] Differences in NPGO winter wind patterns have a strong signature on the CUI, and they significantly influence the upwelling season onset off central California: the NPGO+ upwelling season starts about 6 weeks earlier than in NPGO−. This difference in upwelling season onset has a large impact on the TUMI: the wintertime wind amplitude difference is responsible for half of the NPGO+/NPGO− difference in TUMI (Figure 2). During the rest of the upwelling season, wind differences between both NPGO phases are weak and not significant (statistically) although their cumulative effect explains the other half of the TUMI difference.

[14] Time series correlations over the 42 year-long period from 1967 to 2008 generally confirm these findings. STI and TUMI variability is significantly correlated with the NPGO in the central CCS (with correlation coefficients 0.37 and 0.61 respectively, see Figure 3 and *Di Lorenzo et al.* [2008] for the calculation), but not in the southern and northern CCS. In the central CCS, NPGO+ (NPGO−) years are thus associated with early (late) onset of the upwelling season and stronger (weaker) overall upwelling winds.

4. Impact on the Ecosystem

[15] The biological consequences of spring transition variability are worth investigating because of the importance of phenology for higher trophic levels. For this purpose, we couple a regional ocean model (ROMS, the Regional Ocean Model System) [*Shchepetkin and McWilliams*, 2005] to NEMURO (North Pacific Ecosystem Model for Understanding Regional Oceanography) [*Kishi et al.*, 2007], which is a complex Nutrient-Phytoplankton-Zooplankton-Detritus (NPZD) model (2 sources of nutrients, 2 phytoplankton species, 3 zooplankton species and several detritus pools).

[16] The physical model configuration is the same as that by *Capet et al.* [2008] with a 15-km horizontal resolution. It is forced using two different synthetic wind forcing fields derived from climatological QuikSCAT satellite scatterometer data and restoring the SST to Advanced Very High Resolution Radiometer (AVHRR) measurements. The two monthly-mean synthetic wind fields were built to fit the differences between NPGO+ and NPGO− diagnosed during the wintertime (see section 2 and Figure 1). The two fields differ only from December to March (see auxiliary material)[1]. The winter wind forcing disparity corresponds to a difference of about 10% in TUMI (not shown). The twin experiments are started after a common 12-year-long spin-up and last 24 years. For both phases of the NPGO, Figure 4 shows the mean annual cycle (averaged over the 12 last years of each experiment) of the concentrations of nitrate, total Chl-a and total zooplankton, averaged off the central CCS (34.5°N to 40°N), inshore (from the coast to 150 km offshore) and offshore (from 300 to 450 km from the coast), both 100 m depth.

[17] NEMURO has been calibrated to reproduce a reasonable climatological seasonal cycle compared with data in the CCS. General patterns of the twin simulations are in agreement with the main characteristics of the dynamics of the CCS (Figure 4b), albeit with a low Chl-a bias (also present in previous studies of the California current ecosystem [*Gruber et al.*, 2006]). The presence of this bias may quantitatively affect our results but not our general conclusions that depend on two components adequately captured by the model (undergoing study): a coastal source of nutrients modulated by the seasonal cycle of the dynamics; an offshore conveyor-belt along which a nutrient perturbation (e.g., related to a wind perturbation) can be transferred up the trophic chain.

[18] When the winds are different (shaded area in Figure 4), NPGO+ nitrate, Chl-a, and zooplankton biomass concentrations near the coast are larger than in the NPGO− simulation. At the end of winter, the NPGO+ coastal concentrations of nitrate, Chl-a and zooplankton are larger than in NPGO− by about 25, 15 and 20%, respectively. This enhanced total coastal biomass (Figures 4b and 4c) results

[1]Auxiliary materials are available in the HTML. doi:10.1029/2011GL049966.

Table 1. Linear Correlation Coefficients Between the Indices of Two Pacific Climate Modes of Variability and the Regional Cumulative Upwelling Index[a]

	Reversed STI		TUMI	
	NPGO	PDO	NPGO	PDO
Northern	0.32	**−0.31**	−0.27	**−0.48**
Central	**0.37**	−0.28	**0.61**	**−0.46**
Southern	- - -	- - -	0.29	**−0.40**

[a]Indices have been yearly averaged. Bold numbers indicate correlations significant at the 95 % level or higher.

from an early and more vigorous upwelling-favorable wind season which leads to higher than normal concentrations of nutrients (e.g., nitrate) in the euphotic zone at the beginning of the year (Figure 4a). The offshore region is also strongly affected by this delayed coastal upwelling season and, at the end of winter, Chl-a, and zooplankton concentrations are about 15 and 75% higher in NPGO+ than in NPGO−. Differences observed for offshore nitrate concentrations are not significant. From nutrients to higher trophic levels, coastal biomass concentrations reach successively their maximum between the end of June and the end of July with a lead of about 5 days of NPGO+ over NPGO−. During July, NPGO+ and NPGO− coastal concentrations of Chl-a and zooplankton become quite the same whereas offshore concentrations are still different with NPGO+ concentrations larger of about 13 and 20% than in NPGO−. NPGO+ and NPGO− offshore concentrations become again the same at the end of September.

[19] These results show that according to the NPGO phase, a delayed coastal upwelling induced by delayed upwelling favorable winds significantly impacts both on the timing of the biological cycle and on the productivity of the ecosystem. This is true not only at the coast but also offshore, where differences are surprisingly more important in proportion and last longer. Moreover, irrespective to the offshore distance, a 10% net difference in the TUMI implies 10% and 8% biomass differences in Chl-a and zooplankton biomass, respectively. Finally, the combination of cross-shore transport and the regeneration loop may explain strong differences in the ecosystem functioning between the two NPGO phases as it will be shown in a subsequent paper.

5. Conclusion

[20] We have shown that the NPGO is related to winter atmospheric variability mainly in the central part of the CCS leading to a delayed upwelling response. Recent studies show that in the central tropical Pacific and during boreal winter, SST anomalies associated with the evolution of the central Pacific El Niño excite variability in the atmospheric NPO, which in turn drives the oceanic NPGO [*Di Lorenzo et al.*, 2010]. This dynamical chain from central tropical Pacific to NPGO explains over 75% of the low-frequency variability of the NPGO. It is known that ENSO, and in particular the canonical eastern Pacific El Niño, excites an atmospheric and oceanic teleconnection to the CCS that affects upwelling by both modulating the depth of the coastal thermocline [*Lynn and Bograd*, 2002] and driving variability in the coastal upwelling winds connected to the PDO [*Schneider and Cornuelle*, 2005]. Our results expand this view by highlighting the strong dynamical link that exists between the central tropical Pacific El Niño and the intensity and phase of upwelling along California's coast. Together, these findings suggest that tropical Pacific variability and its northern hemisphere expression in the NPGO exert an even stronger control on upwelling along the central part of California's coast than previously reported. In accord with this view, the variability of the seasonal upwelling onset and the variability of the upwelling efficiency in the CCS are not solely captured by the NPGO but also by the PDO. Table 1 gives the linear correlation coefficients between these two climate modes and the seasonal upwelling indexes (STI and TUMI) in the three subregions of the CCS defined in section 3. The seasonal upwelling variability in the central CCS is mainly captured by the NPGO (0.61 and 0.37 significant coefficients for TUMI and reversed STI, respectively). Moreover, correlation of STI with PDO is not statistically significant in this region. Conversely, the variability in the northern CCS is mainly captured by the PDO (−0.31 and 0.48, for correlation with reversed STI and TUMI, respectively). This is coherent with the predominant regional signature of each climate mode [*Chhak and Di Lorenzo*, 2007; *Di Lorenzo et al.*, 2008].

[21] We tested numerically the effects of differences observed between NPGO+ and NPGO− wintertime situations on a planktonic ecosystem. We found that delayed upwelling favorable winds influence on the availability of nutrients and on the productivity of lower trophic levels of the ecosystem from the coast to the offshore region. This highlights the importance of wintertime upwelling on biological production in the CCS and complements the conclusions of recent studies focused on higher trophic levels [*Black et al.*, 2010; *Dorman et al.*, 2011]. In an early upwelling scenario (NPGO+), the ecosystem is more productive around the year than in a late upwelling scenario (NPGO−). Our results are corroborated by observations in 2005 (a NPGO− year) with a late upwelling onset [*Schwing et al.*, 2006] and 2007 (a NPGO+ year) with an early upwelling onset [*McClatchie et al.*, 2009]. For instance, the observed 2005 3-week-delay in the upwelling onset was responsible for a late spring bloom and disrupted the development of higher trophic level species (e.g., zooplankton, rockfish and seabirds) [*Mackas et al.*, 2006; *Henson and Thomas*, 2007]. On the contrary, 2007 was characterized by a 6-week-early upwelling season leading not only to anomalous high concentration in nitrate and Chl-a, but also in zooplankton and fish species typical of cool conditions [*McClatchie et al.*, 2009]. Our numerical experiments also highlight the strength and time persistence of perturbations from coastal origin in the offshore region: surprisingly, the productivity of the ecosystem is, in proportion, more affected offshore than nearshore. The wind analysis carried out in this study suggests that a more complete assessment of the link between the NPGO and the functioning of the CCS ecosystem should account for NPGO-induced perturbations in prey-predator match/mismatch.

[22] **Acknowledgments.** We acknowledge the support of the INSU-CNRS CYBER-LEFE programme through the TWISTED action, the French Ministry of Research, Université Européenne de Bretagne, NSF CCE-LTER and GLOBEC OCE-0815280. We also thank Vincent Combes for the discussions we had with him.

[23] The Editor thanks two anonymous reviewers for their assistance in evaluating this paper.

References

Alexander, M. A., I. Bladé, M. Newman, J. R. Lanzante, N. C. Lau, and J. Scott (2002), The atmospheric bridge: The influence of ENSO teleconnections on air-sea interaction over the global oceans, *J. Clim.*, *15*, 2205–2231.

Ashok, K., C.-Y. Tam, and W.-J. Lee (2009), ENSO Modoki impact on the Southern Hemisphere storm track activity during extended austral winter, *Geophys. Res. Lett.*, *36*, L12705, doi:10.1029/2009GL038847.

Bakun, A. (1973), Coastal upwelling indices, west coast of North America, 1946–71, *NOAA Tech. Rep. NMFS SWFSC 671*, 114 pp., NOAA, Seattle, Wash.

Barth, J. A., et al. (2007), Delayed upwelling alters nearshore coastal ocean ecosystems in the northern California Current, *Proc. Natl. Acad. Sci. U. S. A.*, *104*(10), 3719–3724, doi:10.1073/pnas.0700462104.

Black, B. A., I. D. Schroeder, W. J. Sydeman, S. J. Bograd, and P. W. Lawson (2010), Wintertime ocean conditions synchronize rockfish growth and seabird reproduction in the central California Current ecosystem., *Can. J. Fish. Aquat. Sci.*, *67*(7), 1149–1158, doi:10.1139/F10-055.

Bograd, S. J., I. Schroeder, N. Sarkar, X. Qiu, W. J. Sydeman, and F. B. Schwing (2009), Phenology of coastal upwelling in the California Current, *Geophys. Res. Lett.*, *36*, L01602, doi:10.1029/2008GL035933.

Capet, X., F. Colas, J. C. McWilliams, P. Penven, and P. Marchesiello (2008), Eddies in eastern boundary subtropical upwelling systems, in *Ocean Modeling in an Eddying Regime*, *Geophys. Monogr. Ser.*, vol. 177, edited by M. W. Hecht and H. Hasumi, pp. 131–147, AGU, Washington, D. C., doi:10.1029/177GM10.

Chhak, K., and E. Di Lorenzo (2007), Decadal variations in the California Current upwelling cells, *Geophys. Res. Lett.*, *34*, L14604, doi:10.1029/2007GL030203.

Chhak, K. C., E. Di Lorenzo, N. Schneider, and P. F. Cummins (2009), Forcing of low-frequency ocean variability in the northeast Pacific, *J. Clim.*, *22*(5), 1255–1276, doi:10.1175/2008JCLI2639.1.

Di Lorenzo, E., et al. (2008), North Pacific Gyre Oscillation links ocean climate and ecosystem change, *Geophys. Res. Lett.*, *35*, L08607, doi:10.1029/2007GL032838.

Di Lorenzo, E., et al. (2009), Nutrient and salinity decadal variations in the central and eastern North Pacific, *Geophys. Res. Lett.*, *36*, L14601, doi:10.1029/2009GL038261.

Di Lorenzo, E., K. M. Cobb, J. C. Furtado, N. Schneider, B. T. Anderson, A. Bracco, M. A. Alexander, and D. J. Vimont (2010), Central Pacific El Niño and decadal climate change in the North Pacific Ocean, *Nat. Geosci.*, *3*, 762–765, doi:10.1038/ngeo984.

Dorman, J. G., T. M. Powell, W. J. Sydeman, and S. J. Bograd (2011), Advection and starvation cause krill (*Euphausia pacifica*) decreases in 2005 Northern California coastal populations: Implications from a model study, *Geophys. Res. Lett.*, *38*, L04605, doi:10.1029/2010GL046245.

Gruber, N., H. Frenzel, S. Doney, P. Marchesiello, J. Mcwilliams, J. Moisan, J. Oram, G. Plattner, and K. Stolzenbach (2006), Eddy-resolving simulation of plankton ecosystem dynamics in the California Current system, *Deep Sea Res., Part I*, *53*(9), 1483–1516, doi:10.1016/j.dsr.2006.06.005.

Henson, S. A., and A. C. Thomas (2007), Interannual variability in timing of bloom initiation in the California Current System, *J. Geophys. Res.*, *112*, C08007, doi:10.1029/2006JC003960.

Kalnay, E., et al. (1996), The NCEP/NCAR 40-year reanalysis project, *Bull. Am. Meterol. Soc.*, *77*(3), 437–471.

Kishi, M., et al. (2007), NEMURO a lower trophic level model for the North Pacific marine ecosystem, *Ecol. Modell.*, *202*(1–2), 12–25, doi:10.1016/j.ecolmodel.2006.08.021.

Kruskal, W. H., and W. A. Wallis (1952), Use of ranks in one-criterion variance analysis, *J. Am. Stat. Assoc.*, *47*(260), 583–621, doi:10.2307/2280779.

Linkin, M. E., and S. Nigam (2008), The North Pacific Oscillation west Pacific teleconnection pattern: Mature-phase structure and winter impacts, *J. Clim.*, *21*(9), 1979–1997, doi:10.1175/2007JCLI2048.1.

Lynn, R., and S. Bograd (2002), Dynamic evolution of the 1997–1999 El Niño-La Niña cycle in the southern California Current System, *Prog. Oceanogr.*, *54*(1–4), 59–75, doi:10.1016/S0079-6611(02)00043-5.

Mackas, D. L., W. T. Peterson, M. D. Ohman, and B. E. Lavaniegos (2006), Zooplankton anomalies in the California Current system before and during the warm ocean conditions of 2005, *Geophys. Res. Lett.*, *33*, L22S07, doi:10.1029/2006GL027930.

Mantua, N. J., S. R. Hare, Y. Zhang, J. M. Wallace, and R. C. Francis (1997), A Pacific interdecadal climate oscillation with impacts on salmon production, *Bull. Am. Meterol. Soc.*, *78*(6), 1069–1079.

McClatchie, S., et al. (2009), The state of the California Current, 2007–2008: La Niña conditions and their effects on the ecosystem, *CalCOFI Rep.*, *49*, 39–76.

Schneider, N., and B. D. Cornuelle (2005), The forcing of the Pacific Decadal Oscillation, *J. Clim.*, *18*(21), 4355–4373, doi:10.1175/JCLI3527.1.

Schwing, F. B., M. O. Farrell, and J. M. Steger (1996), Coastal Upwelling indices west coast of North America, *NOAA Tech. Rep. NMFS SWFSC 231*, 144 pp., NOAA, Seattle, Wash.

Schwing, F. B., N. A. Bond, S. J. Bograd, T. Mitchell, M. A. Alexander, and N. Mantua (2006), Delayed coastal upwelling along the U.S. West Coast in 2005: A historical perspective, *Geophys. Res. Lett.*, *33*, L22S01, doi:10.1029/2006GL026911.

Shchepetkin, A., and J. Mcwilliams (2005), The regional oceanic modeling system (ROMS): A split-explicit, free-surface, topography-following-coordinate oceanic model, *Ocean Modell.*, *9*(4), 347–404, doi:10.1016/j.ocemod.2004.08.002.

B. Blanke and X. Capet, Laboratoire de Physique des Océans, UMR 6523, Université de Bretagne Occidentale, IFREMER, 6 avenue Le Gorgeu, CS 93837, F-29238 Brest CEDEX 3, France. (bruno.blanke@univ-brest.fr; xavier.capet@ifremer.fr)

F. Chenillat and P. Rivière, Laboratoire des Sciences de l'Environnement Marin, UMR 6539, Université de Bretagne Occidentale, Institut Universitaire Européen de la Mer, Place Nicolas Copernic, F-29280 Plouzané CEDEX, France. (fanny.chenillat@univ-brest.fr; pascal.riviere@univ-brest.fr)

E. Di Lorenzo, School of Earth and Atmospheric Sciences, Georgia Institute of Technology, Atlanta, GA 30332-0340, USA. (edl@eas.gatech.edu)